A fast and efficient algorithm for time synchronization in satellite quantum key distribution

A V Miller

Moscow Centre for Quantum Technologies, Moscow, Russia

E-mail: avm@mcqt.ru

Abstract. Time synchronization is one of the most crucial issues that must be addressed in developing quantum key distribution (QKD) systems. It not only lets the transmitter and the receiver to assign a sequence number to each event and then do correct basis reconciliation, but also allows to increase signal-to-noise ratio. Time synchronization in satellite communications is especially complicated due to such factors as high loss, signal fading and Doppler effect. In this work, a simple, efficient and robust algorithm for time synchronization is proposed. It was tested during experiments on QKD between Micius, the world's first quantum communications satellite, and an optical ground station located in Russia. The obtained synchronization precision lies in the range from 467 to 497 ps. The authors compare their algorithm for time synchronization with the previously used methods. The proposed approach can also be applied to terrestrial QKD systems.

1. Introduction

The idea of quantum cryptography is not based on computational complexity of mathematical algorithms, but on the laws of physics. The idea was first announced in 1984 by Bennett and Brassard, who proposed the first quantum cryptography protocol, BB84 [1]. An experimental implementation of quantum key distribution was first demonstrated in 1989 [2]. In that experiment, qubits were encoded in photon's polarization and the photons were transmitted through 32.5 cm on an optical table. Since then, the technology has been widely developed. In particular, distance between shared parties has increased significantly. Thus, free-space QKD over 144 km was experimentally demonstrated using decoy-state BB84 protocol [3]. Recently, using twin-field QKD protocol, quantum key exchange through optical fiber over to 833.8 km was implemented [4]. Although the obtained results are outstanding in terrestrial QKD, secret key rate is of ~10^{-2} bit/s, which is barely attractive from the point of view of practical applications. The only reasonable way to build a truly global, intercontinental, quantum network to date is using of artificial satellites as trusted nodes between remote ground stations. In 2016, the first such satellite, Micius, was launched into its orbit, which was followed by experiments on satellite-to-ground QKD [5–7], entanglement distribution [8], entanglement-based QKD [9] and quantum teleportation [10].

Time synchronization is one of the most crucial factors in distributing a quantum key. It not only allows Alice and Bob to assign an absolute sequence number to each event and then do correct basis reconciliation. Also, precise synchronization can significantly increase signal-to-noise ratio. In satellite QKD, synchronization is especially complicated due to such factors as signal fading, high loss and Doppler effect. In QKD systems, synchronization can be implemented, for instance, by means of electrical signal [11] or a global navigation satellite system (GNSS) [3]. The most common method is

light synchronization, which implies transmitting intense light pulses at the same wavelength [12] or at a different one [5,13–16]. Also, there is an elegant solution that is based only on analysis of detected quantum signal and does not require any additional hardware [17]. Recently, this approach was successfully adopted to real satellite-to-ground QKD [18]. A similar method had been utilized by another team although the intensity of optical signal was of several orders of magnitude higher than one that corresponds to a single photon level [19]. In this work, we propose another approach, which is more simple to implement and does not require any complex mathematical calculations. It was shown to provide at least 1.5 better synchronization accuracy than previously used methods at processing data from a whole quantum communication session.

The structure of this paper is as follows: in section "Theory", we provide a general description of the problem of synchronization and a detailed description of our algorithm; in section "Experiment and Results", we present experimental data obtained using our synchronization method during QKD between Micius satellite and an optical ground station (OGS) at Zvenigorod observatory; finally, we draw inferences in section "Conclusions".

2. Theory

2.1. Formulation of the problem

Let Alice send quantum states with a period of T_q so that photon i is released at time $T_q \cdot i$. Since Alice's clock can be fast or slow, actual time of photon emission is $\frac{\nu_0}{\nu_A} \cdot T_q \cdot i$. Here, the following notations are introduced: ν_A is the frequency of Alices's clock and ν_0 is the frequency of an absolutely accurate clock. In general, there can be a time offset t_0^A and emission time t_i has therefore to be written as

$$t_i = t_0^A + \frac{\nu_0}{\nu_A} \cdot T_q \cdot i \tag{1}$$

It should be noted that equation (1) implies that ν_A does not depend on time. Generally, the frequency of Alice's clock can change with time: $\nu_A = \nu_A(t)$. Thus, in the most general case, instead of (1), one must write

$$\frac{1}{\nu_0} \int_{t_0^A}^{t_i} \nu_A(\eta) d\eta = T_q \cdot i \tag{2}$$

The aspects related to clock drift will be discussed later in this article. Hereinafter, we assume, unless otherwise specified in the text, that the frequencies of Alice's and Bob's clocks change slowly enough so that these changes can be neglected in considered time intervals.

Since Alice and Bob are spatially separated, there is some signal propagation time t_p. Consequently, Bob receives photons at times t_i^R determined by the following expression:

$$t_i^R = t_0^A + \frac{\nu_0}{\nu_A} \cdot T_q \cdot i + t_p \tag{3}$$

As Bob uses his own clock with a frequency of ν_B and a time offset of t_0^B, he expects to receive photon i at time

$$t_i^{R,EXP} = t_0^B + \frac{\nu_0}{\nu_B} \cdot T_q \cdot i \tag{4}$$

It is obvious that the discrepancy between $t_i^{R,EXP}$ and t_i^R should at least not exceed $\frac{T_q}{2}$. Otherwise, Bob assigns indexes to received photons incorrectly.

If Alice and Bob have adjusted their clocks so that $t_0^B = t_0^A + t_p$, i.e. the 1st photon ($i = 0$) comes exactly at the moment when Bob is waiting for it, the difference between $t_i^{R,EXP}$ and t_i^R is written as

$$t_i^{R,EXP} - t_i^R = T_q \cdot i \cdot \nu_0 \cdot \left(\frac{1}{\nu_B} - \frac{1}{\nu_A}\right) \tag{5}$$

Since $\left|t_i^{R,EXP} - t_i^R\right|$ should be less than $\frac{T_q}{2}$, if taking (5) into consideration, maximum index i_{MAX} so that quantum key distribution is yet feasible can be found:

$$i_{MAX} \cdot \nu_0 \cdot \left|\frac{1}{\nu_B} - \frac{1}{\nu_A}\right| = \frac{1}{2} \tag{6}$$

Low difference in clock frequencies has not been implied so far. However, in most cases, relative difference is quite small. If one defines ε_A and ε_B as follows:

$$\nu_{A/B} = \nu_0 \cdot \left(1 + \varepsilon_{A/B}\right), \tag{7}$$

$$\varepsilon_{A/B} \ll 1. \tag{8}$$

Thus, i_{MAX} can be expressed from (6) and, if taking into account (7) and (8), it can be written as follows:

$$i_{MAX} = \frac{1}{2|\varepsilon_A - \varepsilon_B|} \tag{9}$$

The upper bound for $|\varepsilon_A - \varepsilon_B|$ is the accuracy of the clocks multiplied by 2 and the value of i_{MAX} can thus be estimated. For instance, if best quartz oscillators, which have an accuracy of ~10^{-7}, were utilized, i_{MAX} would be of ~2.5×10^6. At a repetition rate of quantum states of 100 MHz, this corresponds to a time interval of ~25 ms. It means Alice and Bob have to synchronize their clocks somehow at least once every 25 ms. Using of light pulses for such synchronization is widely used [5,12–16]. Thus, Micius satellite is equipped with a beacon laser generating 0.9 ns light pulses at a repetition rate of ~10 kHz, which also serve synchronization purposes. Theoretically, Alice and Bob could use atomic clocks, which are much more accurate, and thus increase i_{MAX} by several orders of magnitude. However, in satellite communications, this would not make sense due to Doppler effect. If a satellite is moving in its orbit at a speed of v_{SAT}, Doppler shift can be roughly estimated as $\frac{v_{SAT}}{c}$. Thus, it does not make sense to utilize clocks with an accuracy much better than $\frac{v_{SAT}}{c}$, which is ~10^{-5} for artificial satellites. However, if the trajectory of a satellite is known with sufficient accuracy, Doppler shift can be compensated explicitly by subtracting time delays. In this paper, we propose another approach, which is based on a simple and robust algorithm of simultaneous compensation of both clock bias and Doppler shift and does not require the trajectory of a satellite to be known.

2.2. The proposed approach

2.2.1. Description of the synchronization method. It is supposed that there is a sequence of N synchro pulses and Alice records the corresponding emission times t_{iA}, $i = 0 \ldots N-1$. Here and below, subscript A (B) means the marked time is measured with Alice's (Bob's) clock. Using a photodetector, Bob detects synchro pulses sent by Alice. Also, Bob detects single photons and assigns two indexes, i and j, to all detection events: i is the number of the closest synchro pulse followed by the event, and j is the sequence number of the event among all ones that occurred between synchro pulses i and $i+1$: see Fig. 1. Alice sends Bob values of t_{iA} through a public communication channel. So, if he knew $\left(t_{ij} - t_i\right)_A$, he could find quantum state numbers n_{ij} using this expression:

$$n_{ij} = \frac{t_{iA} + \left(t_{ij} - t_i\right)_A}{T_q} \tag{10}$$

Therefore, the task of synchronization is reduced to correct determination of $\left(t_{ij} - t_i\right)_A$.

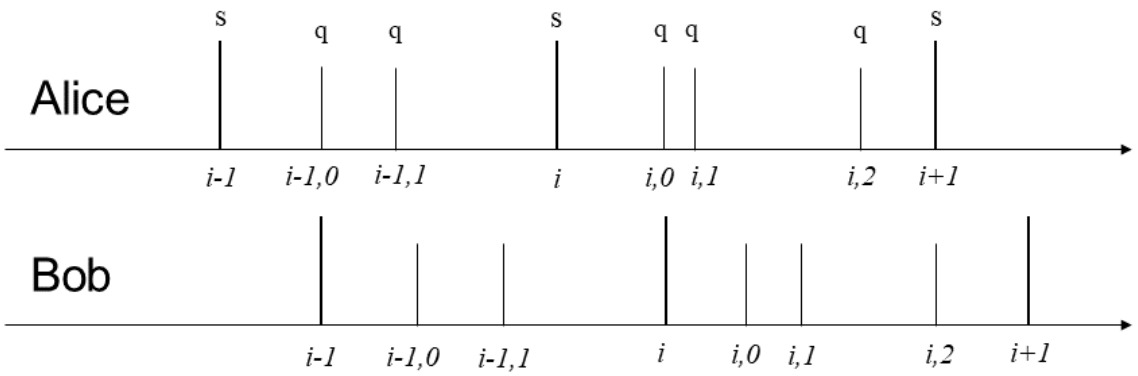

Figure 1. Schematic representation of synchro pulses (s) and quantum signal (q) on the timeline.

First, it is necessary to calculate the time when Bob is receiving synchro pulse i. As Alice and Bob are spatially separated, there is signal propagation time t_p, which depends largely on time in satellite communications. Also, there is a random error δt_i^{rand} caused by imperfection of the measuring equipment, mainly by timing jitter of the photodetector. So, times when Bob receives synchro pulses t_i^R can be written as:

$$t_i^R = t_i + t_p(t_i) + \delta t_i^{rand} \tag{11}$$

Similarly to (11), times when Bob receives quantum states with indexes i, j are written as:

$$t_{ij}^R = t_{ij} + t_p\left(t_{ij}\right) + \delta t_{ij}^{rand} \tag{12}$$

Some point t_k such that all points t_i and t_{ij} lie in some neighborhood of this point $(t_k - \delta t, t_k + \delta t)$ can be considered and $t_p(t)$ can be expanded into Taylor series keeping quadratic terms:

$$t_p(t_i) = t_p(t_k) + t_p'(t_k) \cdot (t_i - t_k) + \frac{1}{2} \cdot t_p''(t_k) \cdot (t_i - t_k)^2 \tag{13}$$

$$t_p\left(t_{ij}\right) = t_p(t_k) + t_p'(t_k) \cdot \left(t_{ij} - t_k\right) + \frac{1}{2} \cdot t_p''(t_k) \cdot \left(t_{ij} - t_k\right)^2 \tag{14}$$

If we subtract (11) from (12) and use expansion (13) and (14), we will get

$$t_{ij}^R - t_i^R =$$

$$= \left(t_{ij} - t_i\right) \cdot \left\{1 + t_p'(t_k) + t_p''(t_k) \cdot (t_i - t_k) + \frac{1}{2} \cdot t_p''(t_k) \cdot \left(t_{ij} - t_i\right)\right\} + \delta t_{ij}^{rand} - \delta t_i^{rand} \tag{15}$$

It is obvious that the 3rd and 4th terms in the curly braces can be discarded if $t_p'' \cdot \delta t \ll t_p'$. Below, we will show that this condition is met during the whole communication time except a negligibly small ($\lesssim$10 ms) area near the moment when the sign of Doppler shift is changing. It should be noted that the 2nd term in the curly braces, t_p', is also extremely small in this area and the change of t_p may therefore not be considered in this area at all. Thus, we are eligible to discard quadratic terms in (15) and, if considering that Alice and Bob use their own clocks for measuring time intervals, (15) can be written as

$$\frac{\nu_0}{\nu_B} \cdot (t_{ij}^R - t_i^R)_B = \frac{\nu_0}{\nu_A} \cdot \left(t_{ij} - t_i\right)_A \cdot \left(1 + t_p'(t_k)\right) + \delta t_{ij}^{rand} - \delta t_i^{rand} \tag{16}$$

Expressing $\left(t_{ij} - t_i\right)_A$ from (16) we will get:

$$\left(t_{ij} - t_i\right)_A = \frac{\nu_A}{\nu_B} \cdot \frac{1}{1 + t_p'(t_k)} \cdot (t_{ij}^R - t_i^R)_B + \frac{\nu_A}{\nu_0} \cdot \left(\delta t_i^{rand} - \delta t_{ij}^{rand}\right) \tag{17}$$

Random errors δt_i^{rand} and δt_{ij}^{rand} are not known, but we can make a reasonable assumption that their expected values are equal to 0. Then, if we introduce notation $C_k = \frac{\nu_A}{\nu_B} \cdot \frac{1}{1+t'_p(t_k)}$, we can write (17) as

$$\left(t_{ij} - t_i\right)_A = C_k \cdot (t_{ij}^R - t_i^R)_B \tag{18}$$

Similarly to (15), for two adjacent synchro pulses, i and $i+1$, we can get

$$t_{i+1}^R - t_i^R = \delta t_{i+1}^{rand} - \delta t_i^{rand} +$$

$$+ (t_{i+1} - t_i) \cdot \left\{1 + t'_p(t_k) + t''_p(t_k) \cdot (t_i - t_k) + \frac{1}{2} \cdot t''_p(t_k) \cdot (t_{i+1} - t_i)\right\} \tag{19}$$

One can consider the following sum: $S_k = \sum_{i=0}^{N-2}\left\{(t_{i+1}^R - t_i^R)_B - (t_{i+1} - t_i)_A\right\}$. On the one hand, it is obvious that

$$S_k = (t_{N-1}^R - t_0^R)_B - (t_{N-1} - t_0)_A \tag{20}$$

On the other hand, using (19) and neglecting quadratic terms again, one can show that:

$$S_k = \frac{\nu_B}{\nu_A} \cdot (t_{N-1} - t_0)_A \cdot (1 + t'_p(t_k)) - (t_{N-1} - t_0)_A + \frac{\nu_B}{\nu_0} \cdot \left(\delta t_{N-1}^{rand} - \delta t_0^{rand}\right) \tag{21}$$

From (20) and (21), we can get

$$(t_{N-1}^R - t_0^R)_B = \frac{\nu_B}{\nu_A} \cdot \left(1 + t'_p(t_k)\right) \cdot (t_{N-1} - t_0)_A + \frac{\nu_B}{\nu_0} \cdot \left(\delta t_{N-1}^{rand} - \delta t_0^{rand}\right) \tag{22}$$

Assuming that the expected values of δt_0^{rand} and δt_{N-1}^{rand} are equal to 0, since $\frac{\nu_B}{\nu_A} \cdot \left(1 + t'_p(t_k)\right) \stackrel{\text{def}}{=} \frac{1}{C_k}$, C_k can be expressed from (22):

$$C_k = \frac{(t_{N-1} - t_0)_A}{\left(t_{N-1}^R - t_0^R\right)_B} \tag{23}$$

C_k is thus found and sequence numbers of quantum states n_{ij} can now be calculated using (10) and (18). Thus, the proposed algorithm is extremely simple for implementing. All that is to be done is to split communication time into short time intervals so that the change of Doppler shift within these time periods can be neglected. Then, it is necessary to find C_k for each time interval using (23) and finally calculate sequence numbers of quantum states.

2.2.2. Synchronization precision. Minimum N. Synchronization precision is a statistical value that can be determined by variance of $(t_{ij} - t_i)_A$. It can be shown that the discrepancy between calculated and true value of $(t_{ij} - t_i)_A$ is

$$\delta\left(t_{ij} - t_i\right)_A = \frac{\nu_A}{\nu_0} \cdot \left(\delta t_{ij}^{rand} - \delta t_i^{rand}\right) +$$

$$+ \frac{\nu_B}{\nu_0} \cdot \frac{(t_{N-1} - t_0)_A}{\left(t_{N-1}^R - t_0^R\right)_B^2} \cdot \left(t_{ij}^R - t_i^R\right)_B \cdot \left(\delta t_0^{rand} - \delta t_{N-1}^{rand}\right) \tag{24}$$

As one can see, the 2nd term in (24) is $\sim \frac{1}{N}$ and it therefore tends to 0 at $N \to \infty$. At the same time, the 1st term does not depend on N. This means that, if N is large enough, we can neglect the 2nd term and only consider the 1st one. If we divide the 2nd component by the 1st one, we will get $\frac{\nu_B}{\nu_0} \cdot \frac{(t_{N-1} - t_0)_A \cdot \left(t_{ij}^R - t_i^R\right)_B}{(t_{N-1}^R - t_0^R)_B^2} \cdot \frac{\delta t_0^{rand} - \delta t_{N-1}^{rand}}{\delta t_{ij}^{rand} - \delta t_i^{rand}}$ or, neglecting small values, $\frac{\left(t_{ij}^R - t_i^R\right)_B}{\left(t_{N-1}^R - t_0^R\right)_B} \cdot \frac{\delta t_0^{rand} - \delta t_{N-1}^{rand}}{\delta t_{ij}^{rand} - \delta t_i^{rand}}$. Since

$\frac{\left(t_{ij}^R - t_i^R\right)_B}{\left(t_{N-1}^R - t_0^R\right)_B} \lesssim \frac{1}{N}$, we can conclude that $N \gtrsim 10$ is sufficient to exclude the 2nd term from consideration. Next, if we assume that δt_i^{rand} and δt_{ij}^{rand} are two independent normally distributed random values, $\delta t_{ij}^{rand} - \delta t_i^{rand}$ is also a normally distributed random value, with expected value of 0 and variance of $\sigma^2 = \sigma_i^2 + \sigma_{ij}^2$, where σ_i is determined by timing jitter of the photodetectors used for detection of synchro pulses at the satellite and at the OGS, whereas σ_{ij} is determined by timing jitter of the single photon detectors used for detection of quantum signal and a finite width of quantum pulses. Thus, the best synchronization precision that can be attained using our method is

$$\sqrt{\sigma_{PD,SAT}^2 + \sigma_{PD,OGS}^2 + \sigma_{SPD}^2 + \sigma_L^2} \tag{25}$$

where $\sigma_{PD,SAT}$ and $\sigma_{PD,OGS}$ characterize timing jitter of the photodetectors used for detection of synchro pulses at the satellite and the OGS correspondingly, σ_{SPD} characterizes timing jitter of the single photon detectors, and σ_L corresponds to the width of quantum pulses.

2.2.3. Maximum N and δt. As we showed above, the area that contains all of N synchro pulses under consideration must be small enough so that we can neglect the change of Doppler shift within this area: $\delta t \ll \frac{t_p'}{t_p''}$ (26). For calculation of $\frac{t_p'}{t_p''}$ we use a simple model. First, we assume that a satellite is moving in a strictly circular orbit (eccentricity = 0). Also, we do not consider Earth rotation since even near the equator the corresponding speed is much less than satellite one. Finally, we only consider a zenith pass. The calculated time dependence of $\frac{t_p'}{t_p''}$ is presented in Fig. 2a. If we consider a sequence with minimum number of pulses, which is $\gtrsim 10$ as was shown above, it corresponds to $\delta t \gtrsim 1ms$ at a repetition rate of synchro pulses of 10 kHz. Then (26) is correct during the whole pass except a small area of $\lesssim 10ms$ near the point where the sign of Doppler shift is changing. However, as one can see in Fig. 2b, Doppler shift is extremely small within this area, $\lesssim 10^{-9}$, and may therefore not be taken into consideration at all.

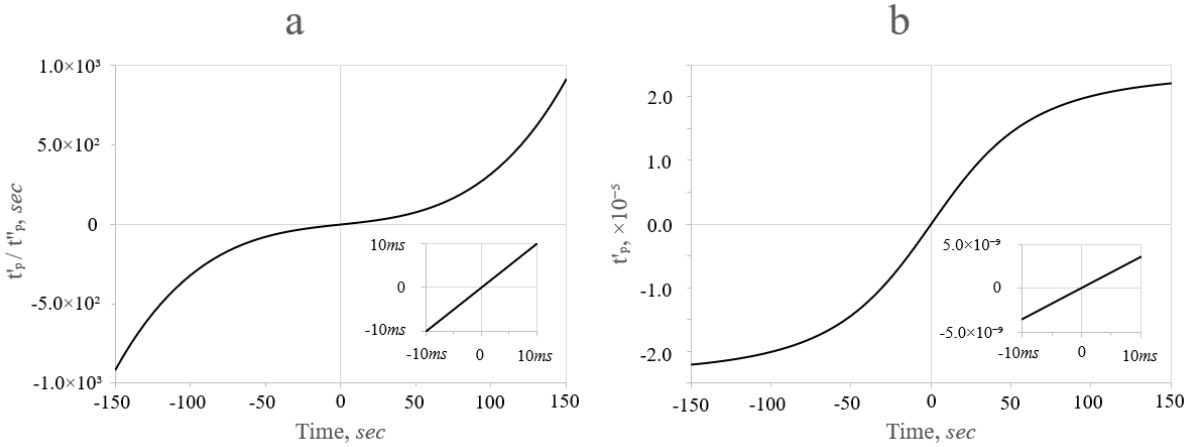

Figure 2. $\frac{t_p'}{t_p''}$ (a) and t_p' (b) during zenith pass of a satellite with an eccentricity of 0 and an altitude of 500 km. Earth rotation is not considered. t_p' and t_p'' are the 1st and the 2nd derivatives of signal propagation time.

2.2.4. Physical meaning of C_k. A low value of clock bias has not been implied so far. However, in most cases, the difference between clock frequencies is relatively small (7,8). The absolute value of

t'_p, which is Doppler shift up to multiplication by -1, does not exceed ~10^{-5} for satellites, i.e. it brings a slight perturbation too. C_k can thus be expanded into Taylor series near 0 keeping only linear terms: $C_k = 1 + \varepsilon_A - \varepsilon_B - t'_p(t_k)$. Thus, at low deviations, $C_k - 1$ characterizes to what extend Alice's clock is fast relative to Bob's one, including Doppler shift.

2.2.5. Reduction to the original method. Minimum possible N that can be in the above algorithm is 2. At $N = 2$, C_k is determined as $\frac{(t_1 - t_0)_A}{(t_1^R - t_0^R)_B}$. Consequently, (18) can be written as $\left(t_{0j} - t_0\right)_A = \frac{(t_1 - t_0)_A}{(t_1^R - t_0^R)_B} \cdot (t_{0j}^R - t_0^R)_B$, which is identical to the main equation of the original synchronization method used by the team of USTC [15]. It should be noted that, at $N = 2$, the 2nd term in (24) becomes comparable with the 1st one and cannot therefore be neglected anymore. Consequently, synchronization precision is distinct from that obtained above for large N.

3. Experiment and results

3.1. Experimental setup

The above algorithm was tested at experiments on QKD between Micius satellite and an OGS at Zvenigorod observatory (55°41'56"N, 36°45'32"E, 180 m above msl). Micius satellite was launched in 2016, after which satellite-to-ground QKD [5–7], entanglement distribution [8], entanglement-based QKD [9], quantum teleportation [10] and some other experiments [20] were carried out. The satellite is equipped with a 530 nm beacon laser that sends 0.9 ns light pulses at a repetition rate of ~10 kHz, which are also used for synchronization purposes. The OGS is a 0.6 m telescope coupled with the rest of optics: mainly, it includes a guide scope with a wide field-of-view camera for course tracking, a fast steering mirror and a narrow field-of-view camera for fine tracking, a dichroic mirror, a spectral filter and a quantum receiver with passive basis selection. Four single photon detectors with a timing jitter of 350 ps FWHM are used for detection of photons in four possible states of polarization. A more detailed description of the OGS can be found in previous publications [21–23].

3.2. The obtained results

A typical time dependence of $C_k - 1$ obtained during a satellite pass is presented in Fig. 3 (gray curve). The obtained coefficients C_k are used for calculation of $\left(t_{ij} - t_i\right)_A$ (18). The corresponding distribution of detection events over time is presented in Fig. 4. In the experiments on QKD, the obtained synchronization precision varies from 536 ps on March 1, 2022 to 593 ps on March 10, 2022. We showed above (25) that the best theoretical value of synchronization precision that can be attained using our algorithm is equal to $\sqrt{\sigma_{PD,SAT}^2 + \sigma_{PD,OGS}^2 + \sigma_{SPD}^2 + \sigma_L^2}$. Since both quantum and synchro signal are detected with single photon detectors of the same type at the OGS, it can be written as

$$\sqrt{\sigma_{PD,SAT}^2 + 2\sigma_{SPD}^2 + \sigma_L^2} \tag{26}$$

The timing jitter of the single photon detectors utilized in the experiments is 350 ps FWHM. The pulse width of quantum signal is 200 ps [5]. If neglecting the timing jitter of the photodetector at the satellite, the best possible synchronization precision is of about 230 ps. As one can notice, the values obtained experimentally are significantly higher. The discrepancy is apparently caused by finite width of synchronization pulses and limited power of synchronization signal. As a result, the detector does not always trigger exactly on the rising edge of a synchro pulse and has some non-zero probability of being triggered during some time behind it. Indeed, it was shown that intensity fluctuations of synchronization light can lead to a significant synchronization error under certain conditions [24]. A detailed study of this phenomenon is beyond the scope of this work and it can be a topic of a separate research.

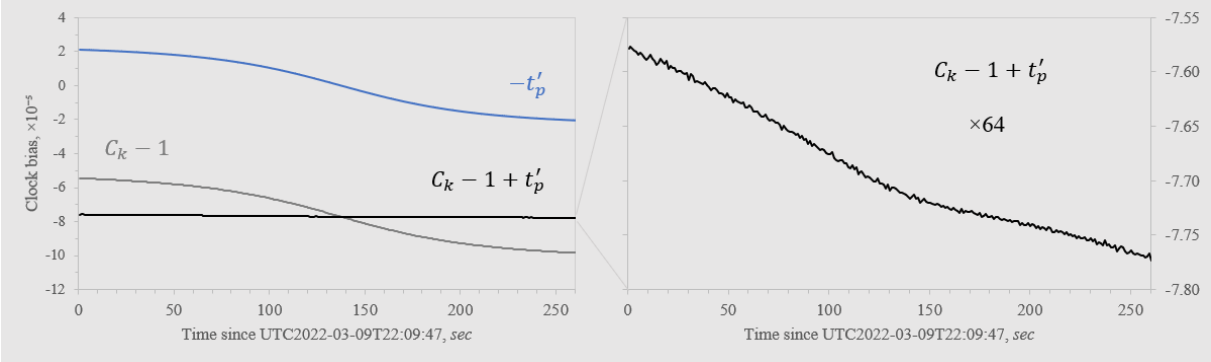

Figure 3. Relative difference between transmitter's and receiver's clock frequencies obtained during QKD on March 9, 2022. Blue curve: Doppler shift calculated from the satellite trajectory determined by means of SGP4 model. Gray curve: $C_k - 1$ determined by analysis of synchro signal. Black curve is obtained by subtracting Doppler shift from $C_k - 1$.

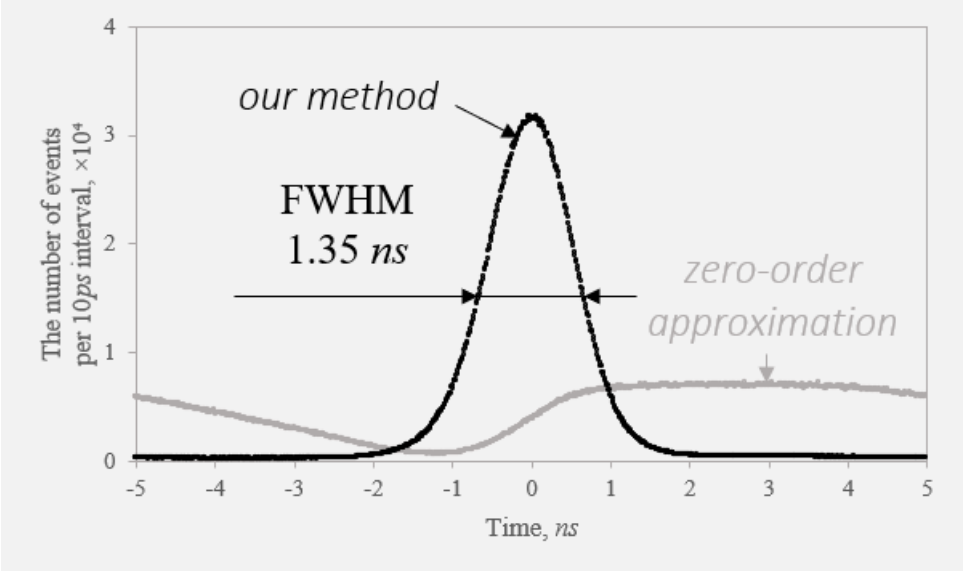

Figure 4. Distribution of events number over time, $rem\left(t_{iA} + \left(t_{ij} - t_i\right)_A + \frac{T_q}{2}, T_q\right) - \frac{T_q}{2}$, during QKD on March 9, 2022. Gray dots – zero-order approximation, $\left(t_{ij} - t_i\right)_A = (t_{ij}^R - t_i^R)_B$. Black dots – our synchronization method. All detection events between UTC2022-03-09T22.09.47 and UTC2022-03-09T22.14.08 (261s) are considered.

As the satellite and the OGS are equipped with GNSS receivers providing a reference clock signal (Pulse-per-Second or PPS), clock bias can be monitored directly analyzing time offsets of PPS tags. Maximum values of speed of clock drift ε_A' and ε_B' observed during the quantum communication sessions are presented in Table 1. One can see that Alice's frequency is changing at least one order of magnitude faster than Bob's one. Also, Alice's frequency is always drifting one direction (decreasing). This is apparently because the clock generator at the satellite is not thermostabilized and is being heated after the electronics starts operating. Nevertheless, maximum speed of clock drift observed in the experiments is at least one order of magnitude less than the rate of Doppler shift change, which is of ~10^{-7} sec^{-1}. As was shown above, the 1st derivative of Doppler shift, equal to the 2nd derivative of signal propagation time, t_p'', is small enough to neglect quadratic corrections and only consider linear terms. Consequently, since the speed of clock drift is $\lesssim 10^{-8}$ sec^{-1}, we can neglect the corresponding quadratic terms as well.

Table 1. Summary of the experiments on QKD between Micius and the OGS at Zvenigorod observatory.

Date	Start time of QKD session, UTC+0	QKD time, *sec*	Elevation asc/desc[a], °	Maximum $\lvert\varepsilon'_A\rvert$, sec^{-1}	Maximum $\lvert\varepsilon'_B\rvert$, sec^{-1}	Synchronization precision, *ps*
March 1, 2022	UTC2022-03-01T22.12.28	222	28.5 / 23.0	7.3×10^{-9}	2.0×10^{-10}	536
March 9, 2022[b]	UTC2022-03-09T22.09.47	261	20.8 / 23.2	7.4×10^{-9}	7.7×10^{-11}	571
March 10, 2022	UTC2022-03-10T21.46.26	249	25.6 / 23.6	7.3×10^{-9}	4.6×10^{-10}	593

[a] Elevation when quantum signal began / ceased to be received
[b] Instead of a truly random sequence, photon states were modulated by a pre-known sequence with a length of 42 949 672 960 states.

Besides the above method for calculation of clock bias, we also use another approach, which is based on analysis of synchro signal. As we showed above, at small deviations, $C_k = 1 + \varepsilon_A - \varepsilon_B - t'_p(t_k)$. Thus, $\varepsilon_A - \varepsilon_B$ can be calculated as $C_k - 1 + t'_p(t_k)$. Coefficients C_k are determined by analysis of synchro signal as was described above, whereas t'_p can be calculated if the trajectory of a satellite is known. We calculate the trajectory of Micius by means of SGP4 model and TLE data taken from sources of free access. As an instance, the time dependencies of $C_k - 1$ (gray curve) and $-t'_p$ (blue curve) obtained on March 9, 2022, are presented in Fig. 3. After subtracting $-t'_p$ from $C_k - 1$, we obtain the black curve, which displays the mutual frequency drift of Alice's and Bob's clocks. In our experiments, during the whole communication time, maximum discrepancy between found thus $\varepsilon_A - \varepsilon_B$ and the same value found by analysis of PPS signal does not exceed 5%.

It should be noted that our algorithm for synchronization does not require any knowledge about the trajectory of a satellite. Using of GNSS receivers is not necessary too. The only purpose of the considerations above is to demonstrate fairness in our assumptions made at the beginning of the paper that frequencies of Alice's and Bob's clocks can be considered as time-independent constants.

3.3. Comparison with other methods

In previous experiments with Micius satellite, when using the original synchronization method, synchronization precision lies in the range 854–1041 ps, whereas for "Qbit4Sync" method, it lies in the range 711–988 ps [18]. As single photon detectors with the same timing jitter are utilized in the experiments, one is eligible to compare the results directly. On average for all satellite passes, our algorithm shows a synchronization precision 1.7 and 1.5 times better than that obtained with the original method and "Qbit4Sync" method correspondingly.

Direct comparison of our algorithm with "Qubit4Sync" method was also carried out at 1s intervals. Applying "Qubit4Sync" algorithm was performed by USTC. The summary of the obtained results is presented in Table 2. As one can notice, synchronization precision at 1s intervals is improved significantly. For our synchronization method, it changes by 15% on average. For the method of USTC, the difference is 1 order of magnitude more, i.e. much more significant. If comparing the two methods with each other at 1s intervals, "Qubit4Sync" demonstrates 1.3 times better accuracy than our algorithm.

Table 2. Direct comparison of the proposed method (MCQT) with "Qubit4Sync" method (USTC) at 1s intervals.

Date	Start of 1s interval, UTC+0	Synchronization precision, *ps*		Sifted key rate, *kbps*		
		MCQT	USTC	MCQT[a]	USTC[b]	Maximum[b]
March 1, 2022	UTC2022-03-01T22.14.40	467	373	13.4	14.1	15.7
March 9, 2022[c]	UTC2022-03-09T22.12.36	480	369	8.58	9.08	10.1
March 10, 2022	UTC2022-03-10T21.48.55	497	380	17.2	18.3	20.4

[a] 2ns time-gate filter is applied.
[b] Calculated under the assumption of a normal distribution
[c] Instead of a truly random sequence, photon states were modulated by a pre-known sequence with a length of 42 949 672 960 states.

We estimated to what extent the difference between the two methods impacts on secret key rate. For our estimations, we made two assumptions. First, the time distribution of error is normal, and second, the same time-gate filter, 2 ns, is applied. According to our calculations, if the algorithm of USTC were used, sifted key rate would increase by no more than 6%: see Table 2 for details. Besides sifted key rate, the change of quantum bit error rate (QBER) should also be taken into account since both parameters affect secret key rate. For instance, QBER obtained at 1s interval since UTC2022-03-09T22.12.36, on March 9, 2022, is of 1.18%. Only 0.54% is due to noise triggering. The other errors, 0.64%, are due to finite polarization extinction ratio caused by imperfection of the optics and are therefore not impacted by signal-to-noise ratio and consequently by synchronization precision. Considering the two assumptions above, one can show that, if the method of USTC were used, error rate due to noise triggering would decrease to 0.51% and the overall QBER would decrease to 1.15%. The change of QBER is thus negligibly small and would therefore not have any significant effect on secret key rate. Thus, under the given conditions, improvement in accuracy by 1.3 times would provide the gain in key rate of only 6%.

4. Conclusions

A simple, efficient and robust algorithm for time synchronization in satellite quantum communications is proposed. It does not imply the trajectory of satellite is known and does not require any complex mathematical calculations. The algorithm was tested during experiments on QKD between Micius satellite and an optical ground station at Zvenigorod observatory. During the experiments, maximum clock bias between Alice's and Bob's clocks, including Doppler shift, was of about 10^{-4}. The obtained synchronization precision does not exceed 0.5 ns.

The results of comparison with other synchronization methods are not unambiguous. At short (1s) time intervals, "Qubit4Sync" method developed by USTC demonstrates 1.3 times better accuracy than our algorithm. Despite this, the gain in quantum key rate does not exceed 6%. If applying our method for processing data from a whole quantum communication session, which typically lasts several hundred seconds, it shows at least 1.5 times better synchronization precision than any of the previously used methods.

The proposed approach implies neither the use of a GNSS, nor even the fact that synchronization pulses and quantum signal must be clocked from the same generator. The authors believe that it can be utilized for time synchronization not only in satellite-based quantum communications but also in terrestrial systems for QKD.

Acknowledgments
The authors are grateful to the University of Science and Technology of China and QSpace Technologies for providing data obtained during their joint experiments. The authors especially thank Dr. Chao-Ze Wang from USTC for his help in processing the experimental data.

References
[1] Bennett C H and Brassard G 1984 *Proc. Int. Conf. of Computers, Systems & Signal Processing (Bangalore)* p. 175
[2] Bennett C H, Bessette F, Brassard G, Salvail L and Smolin J 1992 *J. Cryptol.* **5** 3–28
[3] Schmitt-Manderbach T *et al.* 2007 *Phys. Rev. Lett.* **98** 010504
[4] Wang S *et al.* 2022 *Nat. Photon.* **16** 154–161
[5] Liao S-K *et al.* 2017 *Nature* **549** 43–47
[6] Liao S-K *et al.* 2018 *Phys. Rev. Lett.* **120** 030501
[7] Chen Y-A *et al.* 2021 *Nature* **589** 214–219
[8] Yin J *et al.* 2017 *Science* **356** 1140–1144
[9] Yin J *et al.* 2020 *Nature* **582** 501–505
[10] Ren J-G *et al.* 2017 *Nature* **549** 70–73
[11] Beveratos A, Brouri R, Gacoin T, Villing A, Poizat J-P and Grangier P 2002 *Phys. Rev. Lett.* **89** 187901
[12] Stucki D, Gisin N, Guinnard O, Ribordy G and Zbinden H 2002 *New J. Phys.* **4** 41
[13] Sasaki M *et al.* 2011 *Opt. Express* **19** 10387–10409
[14] Wang S *et al.* 2014 *Opt. Express* **22** 21739–21756
[15] Wang C, Li Y, Cai W, Yang M, Liu W, Liao S and Peng C 2021 *Appl. Opt.* **60** 4787–4792
[16] Shakhovoy R, Puplauskis M, Sharoglazova V, Maksimova E, Hydyrova S, Kurochkin V and Duplinskiy A 2023 *IEEE Journal of Quantum Electronics* **59** 1–10
[17] Calderaro L, Stanco A, Agnesi C, Avesani M, Dequal D, Villoresi P and Vallone G 2020 *Phys. Rev. Appl.* **13** 054041
[18] Wang C-Z, Li Y, Cai W-Q, Liu W-Y, Liao S-K and Peng C-Z 2021 *Opt. Express* **29** 29595–29603
[19] Takenaka H, Carrasco-Casado A, Fujiwara M, Kitamura M, Sasaki M and Toyoshima M 2017 *Nat. Photon.* **11** 502–508
[20] Lu C-Y, Cao Y, Peng C-Z and Pan J-W 2022 *Rev. Mod. Phys.* **94** 035001
[21] Khmelev A V, Duplinskiy A V, Maiboroda V F, Bakhshaliev R M, Balanov M Yu, Kurochkin V L and Kurochkin Yu V 2021 *Tech. Phys. Lett.* **47** 858–861
[22] Khmelev A V, Duplinsky A V, Kurochkin V L and Kurochkin Y V 2021 *J. Phys.: Conf. Ser.* **2086** 012137
[23] Khmelev A V, Ivchenko E I, Miller A V, Duplinsky A V, Kurochkin V L and Kurochkin Y V 2023 *Entropy* **25** 670
[24] Wu Q-L, Han Z-F, Miao E-L, Liu Y, Dai Y-M and Guo G-C 2007 *Opt. Commun.* **275** 486-490